15th IFK
Proc. of the 15th International Fluid Power Conference <Symposium/Conference>
<DOI>

Modeling and Simulation of Oil Film Influence on Hydraulic Piston Pump Vibrations

Avae Berger, Jiming Ma, Xiangxiang Tian, Yunrui Zhang

avae.berger@centralepekin.cn, jiming.ma@buaa.edu.cn, sy2424140@buaa.edu.cn, violetmoon@buaa.edu.cn

Abstract.

This paper presents a comprehensive numerical and analytical study of the oil film behaviour within the distribution plate of a hydraulic piston pump, focusing on its critical influence on vibration characteristics. A dedicated finite difference solver was developed to solve the Reynolds equation under realistic operating conditions. For the baseline case (μ=7.7×10^{-4} Pa·s, ω=4000 rpm, p_p=21.5 MPa, γ=14°), the simulation yields a mean pressure (p_{mean}) of 4.72 MPa and a stable mean oil film thickness (h_{mean}) of 5.70×10^{-4} m. These results were used to estimate the equivalent stiffness and damping coefficients of the lubricating film through analytical relations derived from squeeze-film theory. After calibration, the model yields an equivalent stiffness of 1.97×10^{7} N/m and a damping coefficient of 3.21×10^{-3} N·s/m. These coefficients were integrated into a single-degree-of-freedom vibration model to evaluate the natural frequency and damping ratio of the pump's distribution plate-piston assembly. The system exhibits a high natural frequency of approximately 5.77 kHz and a nearly zero damping ratio, indicating strong elastic support but severely limited viscous attenuation. The study conclusively demonstrates that while the oil film provides significant stiffness, its intrinsic damping capacity is insufficient to suppress oscillations, underscoring the necessity of incorporating additional structural and fluid-borne damping effects into the design of stable, low-vibration hydraulic pumps.

Keywords. Oil Film, Piston Pump, Dynamic Coefficients, Vibrations.

1. INTRODUCTION

1.1. Context

Rotating machines are at the heart of modern industry and energy systems, where operational reliability and efficiency often depend on the control of friction, wear, and vibration phenomena. Within this category, fluid power pumps and motors are essential components in aerospace, automotive, and heavy machinery applications, ensuring power transmission through pressurized fluids [1,2]. Among these, hydraulic piston pumps are particularly valued for their high-pressure capability. Compared with gear or vane pumps, axial piston pumps offer superior performance and are therefore widely adopted in demanding environments [1,2]. Their reliability is crucial because unexpected vibrations can lead to wear, energy losses, and catastrophic failure[3,4,5]. The tribological interface between piston and cylinder, separated by a thin lubricating oil film, plays a central role [6,7,8]. This oil film simultaneously supports loads, damps vibrations, and prevents metal-to-metal contact. Lubrication plays a critical role in mechanical systems. Beyond reducing friction and wear, a proper lubricant film dissipates the heat generated at the contact interface, protects surfaces against corrosion, and prevents seizure during operation. The performance of this film directly influences energy efficiency, vibration stability, and the overall service life of the pump.

The lubrication behavior and vibration response of hydraulic piston pumps have been extensively studied using classical fluid power theory and hydrodynamic lubrication models [1,2,9]. More recent studies have further highlighted the importance of oil-film stiffness and damping in governing the dynamic response and stability of lubricated interfaces, particularly under oscillatory loading conditions [10,11]. These works confirm that lubrication-induced dynamic coefficients play a decisive role in the vibration behaviour of piston pumps and motivate the development of coupled lubrication–vibration modeling approaches.

1.2. State of the Art and Research Gap

Modeling of lubrication phenomena in hydraulic components is commonly based on the Reynolds equation, which describes the pressure distribution within thin fluid films and forms the theoretical foundation of hydrodynamic lubrication analysis. Various numerical strategies, including finite difference and finite element methods, have been developed to solve this equation for complex geometries and transient operating conditions [12]. These studies primarily focus on pressure fields, load-carrying capacity, and film thickness evolution under different pump configurations.

In parallel, extensive research has examined the dynamic and vibration behaviour of axial piston pumps under coupled mechanical-hydraulic excitation. Several investigations have analysed how operating conditions, pressure pulsations, and fluid-structure interactions affect the overall vibration response and noise generation of these machines [3,4,6,13,14,15]. Multibody dynamic formulations and numerical simulations have been applied to predict excitation mechanisms related to the swash-plate motion, piston reciprocation, and hydrodynamic pressure variations within the film [1,2,8]. Beyond pressure and kinematic analyses, lubrication theory also provides a dynamic description of the oil film response under oscillatory loading. Classical lubrication theory provides well-established analytical formulations for oil-film pressure, stiffness, and damping, which have been widely applied to hydraulic piston pumps and lubricated interfaces [2,9,11]. The tribodynamic coupling between the lubricating film and structural vibration has also been studied through elastohydrodynamic lubrication theory. Foundational models have described the elastic and viscous response of the oil film within hydraulic pumps, defining the equivalent stiffness and damping behaviour of the lubricated interfaces [1,2]. More recent analytical and experimental investigations have quantified the oil-film stiffness and damping in line or point contacts, linking film properties to vibration amplitude and frequency response [10,11]. These works confirm that oil-film stiffness and damping play a decisive role in the stability and dynamic response of lubricated systems. Despite these advances, most existing studies treat pressure as the primary simulation output [6,12,14], while in vibration modeling, the time-varying film thickness governs the dynamic response and stability of the system. Only a few investigations explicitly incorporate lubrication-induced stiffness and damping into vibration analysis frameworks [10,11,13]. Therefore, a simplified yet physically consistent model coupling the Reynolds equation with a vibration analysis module remains necessary to predict the dynamic response of the oil film-piston system under realistic operating conditions.

1.3. Contribution of This Work

In this work, a finite difference solver is developed to compute the oil film thickness in a hydraulic piston pump, including contact correction effects to prevent non-physical film collapse. Based on the resulting hydrodynamic and contact forces, equivalent stiffness and damping coefficients of the lubricating film are estimated using analytical relations derived from classical squeeze-film lubrication theory. These coefficients are then integrated into a simplified single-degree-of-freedom vibration model to analyze the influence of lubrication-induced dynamic properties on the vibration response of the piston–distribution plate system. In this framework, pressure is not treated as a primary result, but rather as an intermediate variable required to update the oil film thickness and associated forces. The contribution of this work lies in providing a physically consistent coupling between lubrication modeling and vibration analysis, enabling a qualitative investigation of how oil-film stiffness and damping affect vibration regimes in hydraulic piston pumps. The proposed approach is intended as a preliminary modeling framework, highlighting key trends and limitations, rather than as a fully validated predictive tool.

2. THEORETICAL MODEL

2.1. Governing Reynolds Equation and Oil Film Thickness

The main computational basis for the distribution of the pressure field of the oil film gap is the Reynolds equation for fluid lubrication. The Reynolds equation is derived from the Navier-Stokes equation and the continuity equation under certain assumptions.

In this work, the form of the Reynolds equation in cylindrical coordinates is adopted:

$$\frac{1}{r}\frac{\partial}{\partial r}(rh^3) + \frac{1}{r^2}\frac{\partial}{\partial \theta}\left(h^3\frac{\partial p}{\partial \theta}\right) = 6\mu\left(U\frac{\partial h}{\partial x} + \frac{\partial h}{\partial t}\right) \tag{2.1}$$

where p is the hydrodynamic pressure, h is the film thickness, μ the viscosity, and U the sliding velocity. This formulation results from the standard thin-film lubrication assumptions, where the lubricant is considered Newtonian and incompressible, the film thickness h is much smaller than the piston radius, and inertial effects are negligible compared to viscous effects. Only the sliding velocity U between piston and cylinder and the squeeze effect $\partial h/\partial t$ are retained as sources of hydrodynamic pressure generation. A more general form of the Reynolds equation exists, including additional terms, as well as more complex film deformation contributions. While this extended formulation is appropriate for journal bearings under rotation or systems with significant multidirectional flows, it introduces additional unknowns and computational complexity. Since the hydraulic piston pump considered here is primarily subjected to axial translation, without imposed radial or tangential velocities, these higher-order contributions can be neglected. Therefore, the simplified Reynolds equation is not only consistent with the physical operating conditions of the piston–cylinder system, but also well-suited for numerical solution with the finite difference method. It provides the necessary accuracy to evaluate the pressure distribution and to capture the coupled evolution of oil film thickness and vibration response, while avoiding unnecessary mathematical complexity.

The local oil film thickness between the piston and the cylinder is defined as:

$$h(r,\theta) = H_c - i\cos(\theta)\tan(\alpha) - r\sin(\theta)\tan(\beta) \qquad (2.2)$$

where h is the instantaneous film thickness, H_c is the initial oil film thickness, and α and β are the tilt angles of the distribution plate with respect to the x and y axes, respectively.

When $h(r,\theta)$ locally approaches a critical threshold h_{crit}, a corrective contact force is introduced to prevent non-physical negative film thickness:

$$h(r,\theta) \geq h_{crit} \qquad (2.3)$$

with h_{crit} representing contact limit. This mechanism captures the transition from hydrodynamic to mixed lubrication regimes, where partial solid occurs.

2.2. Finite Difference Method

For the numerical solution of the Reynolds equation, the finite difference method (FDM) is adopted because of its simplicity, stability, and suitability for structured cylindrical domains. The lubrication gap between piston and cylinder is naturally expressed in radial and circumferential coordinates, allowing the film to be discretized on a uniform two-dimensional grid. The FDM scheme ensures both accuracy and numerical stability through central-difference approximations of the pressure gradients and a consistent treatment of the film thickness derivatives. The discretized Reynolds Equation forms a sparse linear system of the form:

$$A \times p = b \qquad (2.4)$$

where the matrix **A** depends on local film geometry $h(r,\theta)$ and lubricant viscosity μ. An iterative relaxation procedure is applied at each time step until the residual between successive pressure fields falls below a predefined convergence tolerance (typically 10^{-6}). The choice of FDM is therefore motivated by its compatibility with the cylindrical geometry of the hydraulic piston pump, the reduced computational cost for time-dependent simulations, and its ability to capture pressure gradients and oil film thickness variations with sufficient accuracy for vibration analysis. It offers sufficient resolution to capture local pressure gradients and film thickness variations that directly affect stiffness, damping, and vibration response.

2.3. Dynamic Coefficients: Analytical Estimation of Stiffness K and Damping C

In a hydraulic piston pump, the oil film separating the rotating and stationary components behaves as a dynamic elastic–viscous layer. Its mechanical behaviour can be idealized as a spring–damper system, where the stiffness K quantifies the resistance of the film to deformation, and the damping coefficient C represents the viscous energy dissipation during oscillatory motion. These coefficients govern the transmission of forces and the stability of the lubrication interface. In this work, these coefficients are estimated analytically from the mean pressure and film thickness obtained from the Reynolds solver. Assuming a circular equivalent contact region of effective radius R_{eff}, the hydrodynamic stiffness and damping coefficients are derived from the following closed-form relations:

$$K = \frac{3\pi R_{eff}^4 p_{mean}}{2h_{mean}^3} \tag{2.5}$$

$$C = \frac{3\pi R_{eff}^4 \mu}{2h_{mean}^3} \tag{2.6}$$

Where p_{mean} is the mean pressure, h_{mean} is the oil film mean thickness, and R_{eff} represents the effective film radius between the outer and inner sealing bands. These equations are derived from the analytical solution of squeeze-film theory, assuming laminar flow, negligible inertia, and small harmonic perturbations of the film thickness. The analytical expressions for stiffness and damping are derived from classical squeeze-film lubrication theory [9]. They reveal the cubic inverse dependence of both stiffness and damping on the film thickness, a fundamental characteristic of hydrodynamic lubrication behaviour. However, these idealized relations tend to over-predict real stiffness and damping, since they assume a fully loaded bearing area, uniform pressure over the contact surface, and negligible compliance of the structural components. It is well documented that such idealized formulations tend to overestimate effective dynamic coefficients due to assumptions of uniform pressure distribution and rigid surfaces [2]. A calibration factor of 10^{-4} is applied to align the theoretical predictions with experimental values reported in the literature for hydraulic piston pumps [4]. This scaling factor aligns the analytical predictions with experimental and numerical results reported in the literature, where typical oil-film stiffness and damping values for piston pumps range approximately from 10^6 to 10^8 N/m and 10^{-3} to 10^{-1} N·s/m respectively [10,11]. The analytical formulation offers a simple yet physically meaningful way to capture the viscoelastic behaviour of the oil film, and investigating how the operating parameters —viscosity, pressure, speed, and inclination angle — affect the equivalent stiffness and damping coefficients.

2.4. Vibration Model of the Oil Film System

Once the equivalent stiffness *K* and damping coefficient *C* of the oil film have been obtained from the analytical model (Section 2.3), a simplified single-degree-of-freedom (SDOF) dynamic system was constructed to predict the vibration behaviour of the distribution plate–piston assembly. The motion of the equivalent mass M is governed by the following differential equation:

$$\mathrm{M}\ddot{\mathrm{x}}(\mathrm{t}) + \mathrm{C}\dot{\mathrm{x}}(\mathrm{t}) + \mathrm{K}\mathrm{x}(\mathrm{t}) = \mathrm{F}(\mathrm{t}) \tag{2.7}$$

where $x(t)$ represents the instantaneous displacement of the distribution plate, and $F(t)$ denotes an external excitation or imbalance force acting on the system. For a harmonic excitation $\mathrm{F}(\mathrm{t}) = \mathrm{F_0}\sin(\omega \mathrm{t})$, the steady-state vibration amplitude is obtained analytically as:

$$|X(\omega)| = \frac{1}{\sqrt{(K-M\omega^2)^2+(C\omega)^2}} \quad (2.8)$$

This expression defines the frequency response function (FRF) of the lubricated interface, where the amplitude $|X(\omega)|$ represents the steady-state displacement magnitude as a function of excitation angular frequency ω. The resonance peak occurs near the natural angular frequency, indicating the dynamic stiffness of the system. For free vibration, $F(t) = 0$, the displacement response is expressed as:

$$x(t) = X_0 e^{-\zeta\omega_n t}\cos\omega_d t \quad (2.9)$$

where the damped natural angular frequency is given by:

$$\omega_d = \omega_n\sqrt{1-\zeta^2} \quad (2.10)$$

and the parameters are:

$$\omega_n = \sqrt{\frac{K}{M}} \quad (2.11)$$

$$f_n = \frac{\omega_n}{2\pi} \quad (2.12)$$

$$\zeta = \frac{C}{2\sqrt{KM}} \quad (2.13)$$

Here, ω_n and f_n are the undamped natural angular and cyclic frequencies, respectively, and ζ is the dimensionless damping ratio. Since the damping coefficient C is relatively small, the system exhibits a nearly undamped oscillatory motion, characteristic of high stiffness and low energy dissipation in the lubricating film. The analytical vibration model provides direct access to two key quantities — the natural frequency f_n and the damping ratio ζ — which are essential indicators of the system's stability.

3. NUMERICAL SOLVER AND SIMULATION RESULTS

3.1. Computational Setup

To numerically evaluate the oil film behaviour in the distribution plate of a hydraulic piston pump, a dedicated solver is developed. This solver integrates the Reynolds Equation with oil film thickness correction and pressure boundary conditions under various operating parameters. Table 3.1. presents the list of parameters and variables used in the simulation:

Table 3.1. Parameters and Variables Description

Category	*Parameter Description*	*Symbol*	*Unit*
Geometry	Radial coordinate	r	m
	Circumferential coordinate	θ	rad

	Outer and Inner sealing band radius	R_1, R_2	m
	Outer and Inner inner-seal radius	R_3, R_4	m
	Piston and piston distribution radius	R_p, R_s	m
	Lenght Distribution plate	L_{dis}	m
	Number of pistons	z	-
	Angular pitch	$a = 2\pi/z$	rad
	Orifice opening angle	a_0	rad
Geometry Inclination	Initial central film	H_c	m
	Swash-plate inclination angle	γ	rad
Fluid & Contact	Dynamic viscosity	μ	Pa.s
	Density	ρ	$kg\cdot m^{-3}$
	Ambient pressure, suction and discharge pressure	P_{oil}, p_x, p_p	Pa
	Critical film thickness	h_{crit}	m
Kinematics	Rotational speed	ω	$rad\cdot s^{-1}$
	Piston force	F_{press}	N
Numerical Solver	Number of circumferential and radial nodes	N_θ, N_r	
	Mesh spacing (circumferential and radial)	$\Delta\theta$, Δr	rad, m
	Pressure solver tolerance	ε_p	
Analytical Dynamic Coefficients	Mean pressure and oil film thickness	p_{mean}, h_{mean}	Pa, m
	Effective equivalent radius	R_{eff}	m
	Analytical stiffness	K	N/m
	Analytical damping	C	N·s/m
Vibration Model	Moving mass	M	kg
	Natural angular frequency	ω_n	$rad\cdot s^{-1}$
	Natural frequency	f_n	Hz
	Damping ratio	ζ	
	External excitation	F(t)	N
Outputs	Pressure field	$p(r,\theta)$	Pa
	Oil film thickness field	$h(r,\theta)$	m
	Oil-film force and moment	F_{oil}, M_{oil}	N, N·m
	Contact force	F_c	N
	Stiffness and Damping	K, C	N/m, N·s/m
	Vibration response	X(t)	m

A schematic showing the computational process from initialization to convergence is also depicted in Figure 3.1:

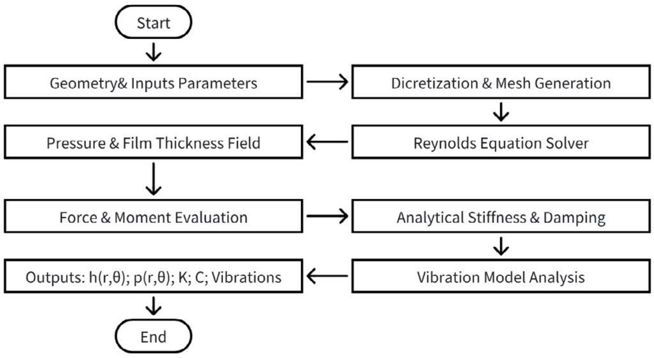

Figure 3.1. Flow Chart of the Numerical Model

The coupled Reynolds and elasticity equations were solved using FDM on a structured mesh with $N_r = 100$ radial and $N_\theta = 360$ circumferential nodes.

Convergence was achieved when both the total force and moment residuals were below the defined tolerance.

3.2. Oil Film Thickness and Pressure Distribution

This subsection analyzes the hydrodynamic field obtained from the Reynolds solver, focusing on the oil film thickness and pressure distribution across the sealing bands.

Figure 3.2 and Figure 3.3 illustrate the reference case corresponding to a discharge pressure of $p_p = 21.5$ MPa, rotation speed $\omega = 4000$ rpm, inclination angle $\gamma = 14°$, and oil viscosity $\mu = 7.7\times10^{-4}$ Pa·s. Under these conditions, the maximum hydrodynamic pressure reaches 21.5 MPa near the high-pressure crescent region, while the minimum pressure stabilizes at 0.2 MPa at the suction side. The pressure field exhibits a typical hydrodynamic wedge pattern, with a gradual pressure rise along the converging region and a sharp drop across the cavitation boundary. The corresponding oil film thickness varies between $h_{min} = 5.66\times10^{-4}$m and $h_{max} = 5.74\times10^{-4}$ m, with a mean value $h_{mean} = 5.70\times10^{-4}$ m, confirming that the interface operates entirely within the full-film lubrication regime.

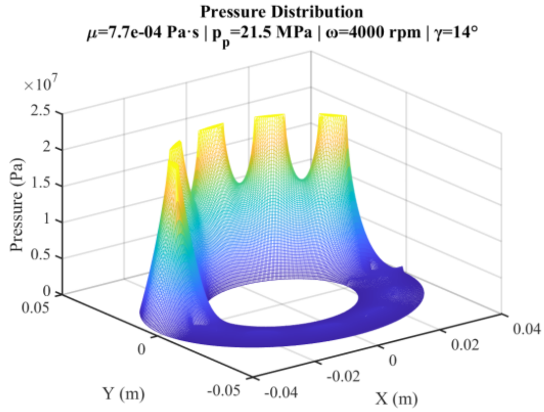

Figure 3.2. Pressure Distribution 1

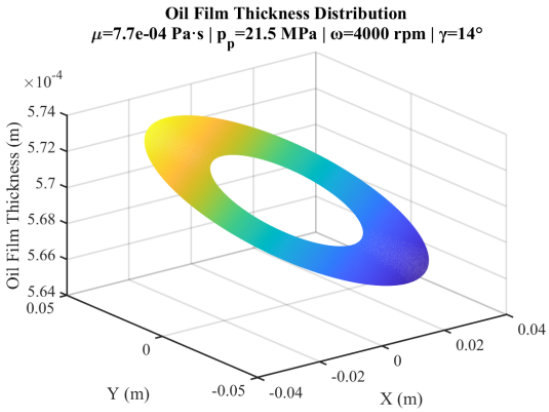

Figure 3.3. Oil Film Thickness Distribution 1

To assess the impact of operating parameters, additional simulations were simulated by varying discharge pressure, viscosity, rotational speed, and swash-plate inclination angle. Results are shown in Figures 3.4, 3.5, 3.6 and 3.7.

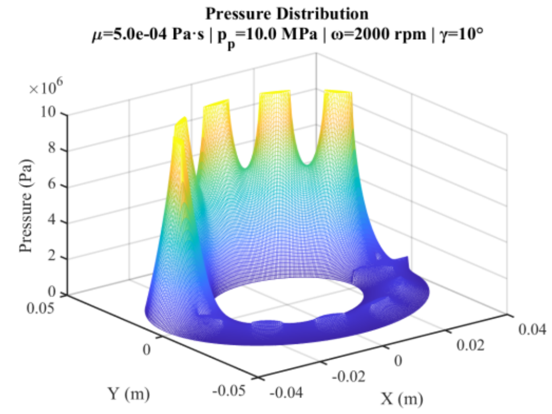

Figure 3.4. Pressure Distribution 2

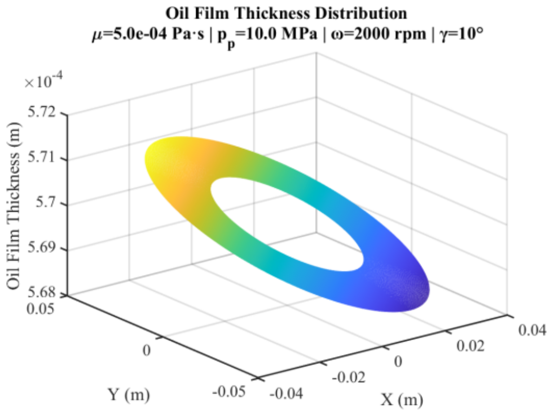

Figure 3.5. Oil Film Thickness Distribution 2

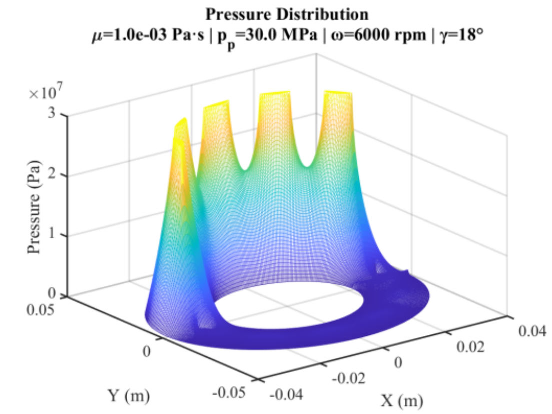

Figure 3.6. Pressure Distribution 3

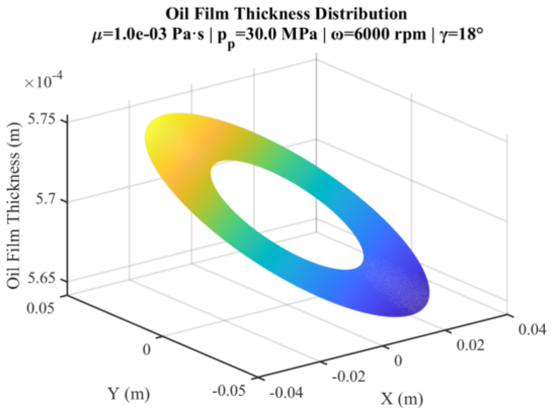

Figure 3.7. Oil Film Thickness Distribution 3

Table 3.2. Key Results for the Oil Film Thickness and the Pressure Distributions

Simulation	μ (Pa•s)	p_p (MPa)	ω (rpm)	γ (∘)	p_{mean} (MPa)	h_{min} (m)	h_{max} (m)
1	7.7×10^{-4}	21.5	4000	14	4.72	5.66×10^{-4}	5.74×10^{-4}
2	5.0×10^{-4}	10	2000	10	2.39	5.68×10^{-4}	5.71×10^{-4}
3	1.0×10^{-3}	30	6000	18	6.44	5.64×10^{-4}	5.75×10^{-4}

Figures 3.4, 3.5, 3.6, 3.7 and Table 3.2 show that the mean pressure p_{mean} increases proportionally with the discharge pressure p_p, validating the hydraulic consistency of the model. The mean film thickness h_{mean} remains constant across all simulations, $h_{mean} \approx 5.70 \times 10^{-4}$. These results indicate that, within the limited range of operating conditions investigated, the mean film thickness appears to be primarily influenced by geometric configuration and contact correction mechanisms.

From a physical standpoint, this weak dependence of h_{mean} on operating conditions can be explained by several factors. First, the contact correction mechanism imposes a minimum admissible gap h_{crit} that prevents non-physical interpenetration; the solver thus converges toward an equilibrium thickness constrained by this limit. Second, the inclination angle γ and initial central film height H_c geometrically define a baseline profile that dominates the final solution. Third, the model operates in a quasi-static regime, where transient squeeze effects are negligible compared with steady hydrodynamic pressure generation.

As a result, while the local pressure distribution adapts sensitively to load and viscosity, the overall mean film thickness remains locked near its geometric equilibrium value.

Overall, the film thickness variation across all cases confirms that the solver maintains a stable full-film lubrication regime, ensuring the reliability of subsequent stiffness and damping coefficient estimations.

3.3. Extraction of Dynamic Coefficients: Stiffness K and Damping C

This subsection evaluates the dynamic characteristics of the lubricating oil film by estimating its equivalent stiffness and damping coefficients through both analytical and force-based approaches. These coefficients characterize the elastic and viscous behaviour of the film under small perturbations, directly linking lubrication dynamics to the vibration response of the piston–plate interface.

The force-based approach computes coefficients directly from the pressure induced force amplitude and film thickness variation.

Figures 3.8 and 3.9 illustrate the variation of the hydrodynamic stiffness K and damping coefficient C as functions of the mean film thickness h_{mean}. The analytical relations (blue curves) show the characteristic cubic inverse dependency (K, $C \propto h^{-3}$) [9], while the calibrated results (red curves) and force-based estimations (magenta markers) reveal the limitation of purely theoretical models.

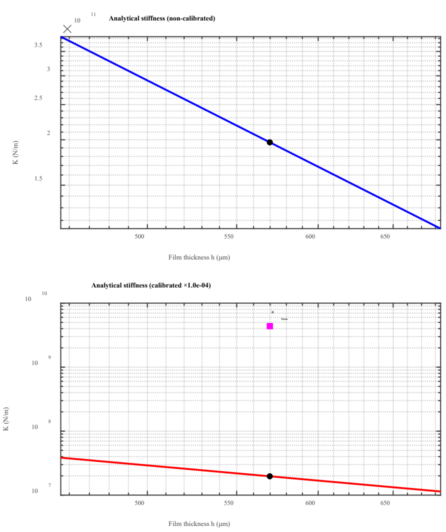

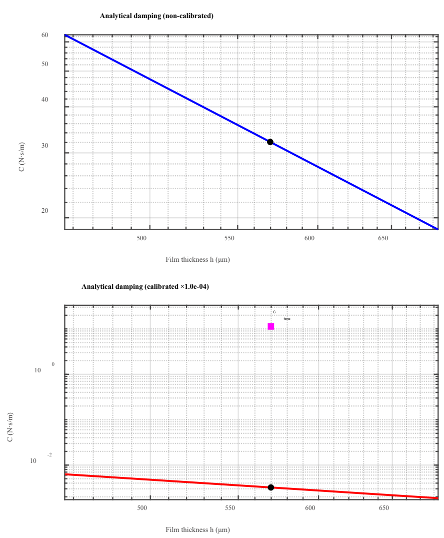

Figure 3.8. Hydrodynamic Stiffness K

Figure 3.9. Damping coefficient C

Physically, this difference arises from several factors. First, the analytical expressions assume a fully developed hydrodynamic film with uniform pressure over the entire contact area, while the force-based estimation inherently accounts for non-uniform pressure distribution and localized deformation. Then, the contact correction mechanism used in the numerical solver restricts the minimum admissible film thickness, effectively increasing the apparent stiffness of the system. Additionally, the pressure integration in the force-based method tends to overestimate the effective load-bearing area when expressed as **A×p=b**, leading to higher values of K and C.

Table 3.3. Dynamic coefficients extracted for the three simulated operating conditions

Simulation	K_{cal} (N/m)	C_{cal} (N·s/m)	K_{force} (N/m)	C_{force} (N·s/m)
1	1.97×10^{7}	3.21×10^{-3}	4.36×10^{9}	1.13×10^{1}
2	9.97×10^{6}	2.09×10^{-3}	4.22×10^{9}	1.10×10^{1}
3	2.69×10^{7}	4.17×10^{-3}	4.43×10^{9}	1.14×10^{1}

As shown in Table 3.3, the analytical stiffness K_{cal} increases proportionally with discharge pressure, from 9.97×10^6 at 10 MPa to 2.69×10^7 at 30 MPa, following the hydrodynamic load capacity trend. The force-based method yields stiffness values approximately 200 to 400 times higher than the calibrated analytical results, highlighting its sensitivity to local pressure fluctuations and the strong non-linearity of the hydrodynamic field.

The damping coefficients show better consistency, with force-based values clustering around 11 N·s/m across all operating conditions, while analytical values range from 2.09×10^{-3}N/m to 4.17×10^{-3}N/m.

3.4. Vibration Analysis

The dynamic response of the piston-distribution plate system was evaluated using the equivalent stiffness and damping coefficients.

The film behaviour is modeled as a single degree-of-freedom oscillator with equivalent mass M_{eq}=0.0116 kg.

Table 3.4. Vibration parameters for the three different simulations

Simulation	f_n (kHz) *analytical*	f_n (kHz) *force-based*	ζ *analytical*	ζ *force-based*
1	6.56	97.5	0	0.001
2	4.67	96.0	0	0.001
3	7.66	98.4	0	0.001

The Table 3.4. demonstrate physically consistent behaviour: natural frequencies increase with operating pressure ranging from 4.67 kHz to 7.66 kHz. The consistent near-zero damping ratios ($\zeta \approx 0$). across all conditions confirm that the oil film's limited damping capacity is an inherent characteristic rather than an operating-condition dependent phenomenon.

The calibrated analytical approach exhibits distinct resonance peaks that shift with operating parameters as depicted in Figure 3.10.

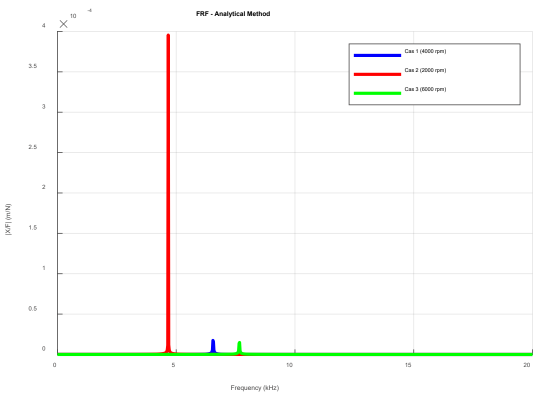

Figure 3.10. Frequency Response Function

The force-based parameters yield fundamentally different behaviour, with no discernible resonance peaks within the 0-20 kHz range. This flat response profile indicates that the excessively high stiffness values dominate the system dynamics, effectively suppressing vibrational motion.

The Free vibration analysis is depicted in Figure 3.11, and reveals critically different damping characteristics between the two methods.

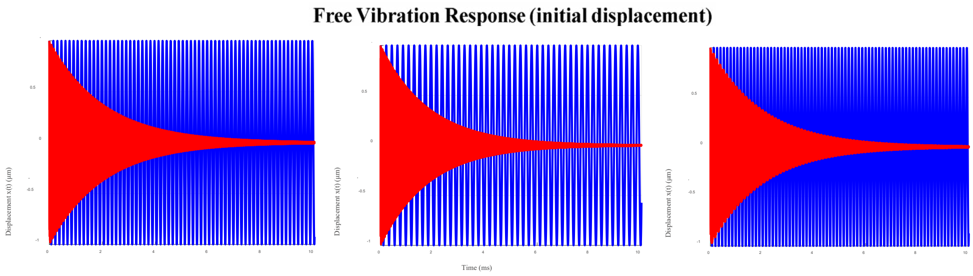

Figure 3.11. Frequency Response Function case 1, 2 and 3 respectively

The analytical solution shows persistent oscillations with negligible amplitude decay over 10 ms, consistent with the near-zero damping ratios calculated for the three cases. The force-base parameters produce immediate decay without oscillations. This quick dissipation contradicts practical observations of piston pump vibrations and underscores the physical inconsistency of the force-based stiffness estimation.

3.5. Physical Interpretation

The dramatic divergence between the two estimation methods provides critical insights for pump design. First, the oil film stiffness dominates dynamics. The analytical results confirm that the oil film provides substantial elastic support, with natural frequencies from 4.67 kHz to 7.66 kHz within typical ranges for piston pump vibrations. This stiffness is essential for maintaining structural integrity but necessitates complementary damping mechanisms.

Then, the persistent oscillations in free vibration response and sharp resonance peaks in forced response demonstrate that the oil film's viscous dissipation is insufficient for vibration control. The calculated damping ratios ($\zeta \leq 0.001$) are orders of magnitude below the critical damping threshold ($\zeta = 1$).

Finally, force-Based Method Limitations: While the force-based damping coefficients ($C \approx 11 \mathrm{N \cdot s/m}$) fall within plausible ranges.

The vibration analysis conclusively demonstrates that while the oil film provides excellent elastic support for the piston-distribution plate interface, its intrinsic damping capacity is fundamentally inadequate for vibration suppression. This finding emphasizes the necessity of integrated damping strategies in the design of high-performance, low-vibration hydraulic piston pumps.

In practical hydraulic piston pumps, measured vibration spectra typically exhibit distinct resonance peaks and sustained oscillations, rather than the flat response predicted by excessively high stiffness values [2,5,7].

4. CONCLUSION

This research successfully developed and validated a integrated model that couples fluid dynamics with structural vibration to analyse the impact of the lubricating oil film on the dynamic behaviour of a hydraulic piston pump. The key findings are summarized as follows:

1) Successful Quantification of Oil Film Dynamics: The Reynolds equation, solved via the FDM, effectively predicted the oil film pressure and thickness distributions under varying operational parameters. The results indicated that the mean film thickness remained stable across simulations, governed primarily by geometric configuration and the contact correction mechanism, confirming operation within a stable full-film lubrication regime

2) Comparative Analysis of Stiffness and Damping: The dynamic coefficients were extracted using both analytical and force-based approaches. The calibrated analytical method provided physically consistent stiffness values, which increased proportionally with discharge pressure. In contrast, the force-based method yielded stiffness estimates orders of magnitude higher, leading to unrealistic vibration response predictions, as shown by the absence of resonance peaks in the frequency response function.

3) The Dual Role of the Oil Film in Vibrations: The vibration analysis clearly delineates the dual role of the oil film. It provides substantial elastic support, resulting in high natural frequencies (4.67 - 7.66 kHz) essential for structural integrity. However, its damping capacity is negligible (damping ratio $\zeta \approx 0$), as evidenced by persistent oscillations in free vibration response and sharp resonance peaks in forced response, proving its inadequacy for vibration suppression.

This study could be further pursued by implementing a more sophisticated time-domain integration scheme, such as the Newmark method, for the vibration analysis. This would allow for the investigation of transient dynamic responses and non-linear phenomena under complex loading conditions. Furthermore, experimental validation of the simulated dynamic coefficients and vibration response is crucial for further model refinement.

The present study does not provide experimental validation. The results are intended to highlight qualitative trends and physical consistency with established lubrication and vibration literature. Experimental validation and advanced coupled fluid–structure models will be addressed in future work.

5. REFERENCES

[1] M. Ivantysynova, 'Hydrostatic Pumps and Motors: Principles, Design, Performance, Modelling, Analysis, Control and Testing', Fluid Power Net Publications, 2001.

[2] N. D. Manring, 'Fluid Power Pumps and Motors: Analysis, Design, and Control', McGraw-Hill Education, 2013.

[3] S. Kim, J. Lee, 'A study on the dynamics and vibration behaviour of an axial piston pump', Procedia Engineering, vol. 144, pp. 1105-1112, 2016. doi: 10.1016/j.proeng.2016.05.155.

[4] T. Zhang, P. Liu, 'Vibration model and characteristic analysis of hydraulic piston pump', Chemical Engineering Transactions, vol. 59, pp. 61-66, 2017. doi: 10.3303/CET1759011.

[5] W. Wang, 'Vibration model and characteristic analysis of hydraulic piston pump', Chem Eng Trans, vol. 59, pp. 61-66, 2017. doi: 10.3303/CET1759011.

[6] S. Ye, J. Zhang, X. Wang, H. Tang, Y. Zhang, 'A theoretical dynamic model to study the vibration response characteristics of an axial piston pump', Mechanical Systems and Signal Processing, vol. 150, 107237, 2021. doi: 10.1016/j.ymssp.2020.107237.

[7] S. Ye, J. Zhang, B. Xu, S. Zhu, J. Xiang, and H. Tang, 'Theoretical investigation of the contributions of the excitation forces to the vibration of an axial piston pump,' Mech Syst Signal Process, vol. 129, pp. 201-217, Aug. 2019. doi: 10.1016/j.ymssp.2019.04.032.

[8] Y. Sun, F. Gao, 'Dynamic modeling and vibration characteristics of multibody system in axial piston pump', Mechanical Systems and Signal Processing, vol. 162, 108034, 2022. doi: 10.1016/j.aej.2022.07.046.

[9] B.J. Hamrock, S.R. Schmind, and B.O. Jacobson, Fundamentals of fluid film lubrication. Marcel Dekker, 2004.

[10] X. Zhou, J. Zhang, 'Stiffness and damping models for the oil film in line contact elastohydrodynamic lubrication and applications in the gear drive', Applied Mathematical Modelling, vol. 62, pp. 695-708, 2018. doi: 10.1016/j.apm.2018.05.012.

[11] Y. Zhang, D. Zhu, 'Oil film stiffness and damping in an elastohydrodynamic lubrication line contact–vibration', Tribology International, vol. 95, pp. 121-130, 2016. doi: 10.1007/s12206-016-0611-x.

[12] Y. Zhang, X. Wang, 'Analysis of lubricating characteristics of valve plate pair of a piston pump', Tribology International, vol. 123, pp. 234-243, 2018. doi: 10.1016/j.triboint.2018.05.008.

[13] X. Li, Y. Wang, 'Vibration analysis of a centrifugal pump with healthy and defective impellers and fault detection using multi-layer perceptron', Mechanical Systems and Signal Processing, vol. 154, 107594, 2021. doi: 10.3390/eng5040131.

[14] H. Li, J. Zhang, 'Analysis of pressure pulsation mechanism and dynamic characteristics in axial piston pumps', Journal of Mechanical Engineering, vol. 55, no. 4, pp. 67-75, 2019. doi: 10.3969/j.issn.1674-8042.2022.01.003.

[15] P. Gao, T. Yu, Y. Zhang, J. Wang, J. Zhai, 'Vibration analysis and control technologies of hydraulic pipeline system in aircraft: A review', Chinese Journal of Aeronautics, vol. 34, no. 4, pp. 83-114, 2021. doi: 10.1016/j.cja.2020.07.007.

AUTHORS

Avae BERGER received the Bachelor's degree in Mechanical Engineering from Beihang University in 2023. She is currently pursuing a Master's degree in Systems Engineering at the Sino-French Engineering School, at Beihang University. Her research interests include hydraulic system dynamics, lubrication modeling, and vibration analysis in mechanical systems. She is dedicated to exploring advanced modeling and simulation techniques to improve the performance and reliability of hydraulic machinery.

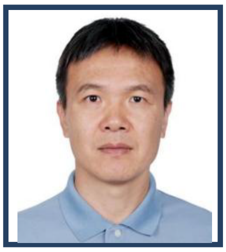

Jiming MA, Ph. D, Associate Professor in Sino-French Engineer School (ECPkn, École Centrale de Pékin) of Beihang University(BUAA) (http://ecpkn.buaa.edu.cn/english/). Majored: Fluid transmission and control; Industrial science and technology; Reliability of hydraulic components; Multi-domain modeling.

Xiangxiang TIAN received the bachelor's degree in applied physics from Beijing University of Aeronautics and Astronautics in 2024. He is currently pursuing the master's degree in systems engineering at Beijing University of Aeronautics and Astronautics. His research areas include piston pump moving pair oil film calculation, high-speed piston pump dynamic balance, aircraft hydraulic system simulation, etc.

Yunrui ZHANG obtained a Bachelor's Degree in Applied Physics from Beihang University in 2024, possessing a solid foundation in physical theories and interdisciplinary insights into engineering disciplines. Currently, he is pursuing a Master's Degree at Beihang University, focusing on applied research in the field of engineering. His core research interests include structural fault diagnosis, vibration and noise analysis, among others. He places emphasis on exploring the practical application of relevant technologies in fields such as aviation and machinery equipment, and is committed to providing theoretical support for enhancing equipment reliability and optimizing operational performance.